Macroscopic Fibers Self-Assembled from Recombinant Miniature Spider Silk Proteins

Margareta Stark,[†,‡] Stefan Grip,[‡] Anna Rising,[‡] My Hedhammar,[†] Wilhelm Engström,[‡] Göran Hjälm,[†,§] and Jan Johansson*[,†]

Department of Anatomy, Physiology, and Biochemistry, The Biomedical Centre, Swedish University of Agricultural Sciences, SE-751 23 Uppsala, Sweden, and Department of Biomedical Sciences and Veterinary Public Health, Swedish University of Agricultural Sciences, SE-750 07 Uppsala, Sweden

Received January 16, 2007; Revised Manuscript Received February 20, 2007

Strength, elasticity, and biocompatibility make spider silk an attractive resource for the production of artificial biomaterials. Spider silk proteins, spidroins, contain hundreds of repeated poly alanine/glycine-rich blocks and are difficult to produce recombinantly in soluble form. Most previous attempts to produce artificial spider silk fibers have included solubilization steps in nonphysiological solvents. It is here demonstrated that a miniature spidroin from a protein in dragline silk of *Euprosthenops australis* can be produced in a soluble form in *Escherichia coli* when fused to a highly soluble protein partner. Although this miniature spidroin contains only four poly alanine/glycine-rich blocks followed by a C-terminal non-repetitive domain, meter-long fibers are spontaneously formed after proteolytic release of the fusion partner. The structure of the fibers is similar to that of dragline silks, and although self-assembled from recombinant proteins they are as strong as fibers spun from redissolved silk. Moreover, the fibers appear to be biocompatible because human tissue culture cells can grow on and attach to the fibers. These findings enable controlled production of high-performance biofibers at large scale under physiological conditions.

Introduction

Dragline silk, one of several different types of silks produced by spiders, is nature's high-performance polymer. It obtains extraordinary toughness from a combination of strength and elasticity,[1] and is also biocompatible.[2] Up to seven specialized glands exist in spiders, producing a variety of silks with different properties.[3] Dragline silk, produced by the major ampullate gland, is the toughest fiber. On a per-weight basis, it outperforms man-made materials such as high-tensile steel and Kevlar.[3,4] Hence, the properties of dragline silk are attractive for the development of new materials for technical and medical purposes. Dragline silk consists of two major polypeptides, referred to as major ampullate spidroin (MaSp) 1 and 2.[5,6] These proteins have apparent molecular masses in the range of 200−720 kDa.[7−9] MaSp1 is more abundant in dragline fibers than is MaSp2,[6,9] and the two proteins are unevenly distributed in the fiber.[10] MaSp1 is found throughout the fiber, while MaSp2 is tightly packed in certain core areas and is missing in the periphery of the fiber. These spidroins are mainly composed of iterated blocks of alternating alanine-rich segments that form crystalline β-sheets in the fiber[6,11] and glycine-rich segments, which are more flexible and appear to lack an ordered structure.[11] The C-terminal region is non-repetitive, conserved between species, and is folded into an α-helical conformation.[12−14] Recently, the N-terminal region of dragline silk proteins has been characterized, revealing a domain that also is highly conserved between different spider species and silk types, and probably is folded into a bundle of α-helices.[15,16]

The African nursery web spider *Euprosthenops australis*, of the Pisauridae family, builds sheet webs for capture of its prey. The mechanical properties of dragline silk vary between species; *Euprosthenops* dragline silk is stiffer, stronger (requires more force to break), and less extendible than dragline silk from species such as *Araneus diadematus* or *Nephila clavipes*.[3,17] Dragline silk from *Euprosthenops* appears to have a greater proportion of crystalline β-sheet structures than silk from *A. diadematus*,[18] most likely due to a higher poly alanine content of MaSp1 from *Euprosthenops* than from other species analyzed to date.[19]

Attempts to produce artificial spider silk have employed natural or synthetic gene fragments that encode parts of dragline silk proteins. Recombinant dragline silk proteins have been expressed in bacteria, yeast, mammalian cells, plants, insect cells, and transgenic goats, but several factors complicate this process.[20−28] Because of the highly repetitive nature of the genes and the concomitant restricted amino acid composition of the proteins, transcription and translation errors occur. DNA fragments encoding spidroins have also been reported to be instable in bacterial hosts.[22,23] Additionally, difficulties have been encountered in maintaining the recombinant silk proteins in soluble form because both natural dragline silk fragments and designed block copolymers easily self-assemble. This causes precipitation of insoluble complexes, protein loss, and requirements for resolubilization procedures.[28,29]

Here, these obstacles are overcome by identifying a minimal spidroin motif that can be readily produced in soluble form in bacteria when fused to a solubility enhancing fusion protein, thioredoxin.[30] Upon release of the fusion partner, the miniature spidrion spontaneously forms silk-like fibers. These are the longest spontaneously formed fibers so far described, using

* Corresponding author. Telephone: +46-18-4714065. Fax: +46-18-550762. E-mail: jan.johansson@afb.slu.se.

† Department of Anatomy, Physiology, and Biochemistry.

‡ Department of Biomedical Sciences and Veterinary Public Health.

§ Present address: Department of Medical Biochemistry and Microbiology, The Biomedical Centre, Uppsala University, SE-751 23 Uppsala, Sweden.

10.1021/bm070049y CCC: $37.00
Published on Web 04/03/2007

recombinant spidroins. Moreover, the fibers show strength and structural characteristics similar to those of regenerated silk and native spider silk, respectively, and seem to be biocompatible to human tissue because they allow tissue culture cell attachment.

Materials and Methods

***E. australis* MaSp1 cDNA Cloning and Sequencing.** Major ampullate glands from approximately 100 adult female nursery web spiders (*E. australis*) were used to construct a custom pDONR222-based CloneMiner cDNA library (Invitrogen, Paisley, UK). cDNA clones encoding the MaSp1 protein were obtained by screening the library with a cDNA probe encoding an alanine- and glycine-rich fragment that originated from *Euprosthenops* spiders of undefined subspecies.[19] Colony blotting and detection were performed using an ECL direct labeling and detection system (GE HealthCare, Uppsala, Sweden) according to the manufacturer's instructions. A single clone (denoted MaSp1 clone 2) was chosen for further analysis. To obtain the full-length sequence of the cDNA insert from this clone, nested deletions were made using the Erase-a-Base System (Promega, Southampton, UK), and sequencing was performed on a MegaBase 1000 instrument (GE HealthCare).

The Expasy tools (www.expasy.org) were applied for analysis of sequence motifs. Turn predictions were done essentially as previously described.[31]

Construction of Recombinant Miniature MaSp1 Genes. All constructs were eventually introduced into a modified pET32 vector encoding a thioredoxin/His-tag/S-tag/thrombin cleavage site/MaSp1 protein. For generation of construct I (see Figure 1B and Supporting Information, Figure 9), a DNA sequence encoding the last four poly-Ala/Gly-rich blocks followed by the non-repetitive C-terminal domain of *E. australis* was amplified by PCR with an Advantage GC2 kit (BD Biosciences, San Jose, CA), using clone 2 as a template. Restriction enzyme recognition sites *Bam*HI and *Hind*III were introduced at the 5′- and 3′-ends, respectively, as well as a stop codon upstream of the *Hind*III site. The resulting construct I was then subcloned into the modified pET32 vector (Merck Biosciences, Darmstadt, Germany), where the original thrombin cleavage site had been removed and a new thrombin site had been introduced downstream of the enterokinase cleavage site.

For the construction of species hybrid constructs, DNA sequences coding for three or four poly-Ala/Gly-rich blocks were amplified by PCR with *LA Taq* (TaKaRa Bio, Saint-Germain-en-Laye, France) in the presence of betaine,[32] using a partial cDNA clone encoding a repetitive region of *Euprosthenops* sp. MaSp1 protein[19] (GenBank entry CQ974358 or CQ816656) as template. Restriction enzyme recognition sites were introduced at the 5′- and 3′-ends, *Nco*I and *Nhe*I, respectively, for clones to be joined to the C-terminal domain, and *Nco*I and *Xho*I, respectively, for clones to be individually expressed with a stop codon inserted directly upstream of the *Xho*I site. A DNA sequence encoding the non-repetitive C-terminal domain was amplified by PCR using a genomic DNA clone encoding a C-terminal MaSp1 domain.[19] This sequence contains also short Ala-rich segments, one with alternating Ala and Ser residues, and the other with six Ala residues (construct V, Figure 1B and Supporting Information, Figure 9). The previously published sequence of this C-terminal domain[19] is nearly identical to the C-terminal domain of *N. clavipes* MaSp1 (95% identity), but quite different from the present *E. australis* sequence (56% identity) (see Supporting Information, Figure 10). Restriction enzyme recognition sites were introduced at the 5′- and 3′-ends, *Nhe*I and *Xho*I, respectively, for clones to be joined to poly-Ala/Gly-rich blocks, and otherwise as described above. The clones containing 4 or 3 poly-Ala/Gly-rich blocks were joined to construct V using the pCR 2.1-TOPO vector (Invitrogen). The resulting constructs II and III were excised with *Nco*I and *Xho*I and subcloned into the modified pET32 vector.

Expression of Recombinant Miniature MaSp1 Proteins and Fiber Formation. The miniature MaSp1 constructs were expressed as fusion proteins, using a modified pET32 vector (see above). The different MaSp1 constructs were used to transform *E. coli* BL21(DE3) cells (Merck Biosciences). The cells were grown at 30 °C in Luria−Bertani medium containing ampicillin to an OD_{600} of 1−1.5, induced with IPTG, and further incubated for 4 h at room temperature. The cells were harvested by centrifugation, incubated with lysozyme and DNaseI in buffer containing 20 mM Tris-HCl (pH 8.0), 20 mM imidazole, and 0.5 M NaCl, and further loaded on Ni-NTA agarose (Qiagen, West Sussex, UK). Bound proteins were eluted from the Ni-NTA column with 200 mM imidazole in buffer containing 20 mM Tris-HCl (pH 8.0) and 0.5 M NaCl and dialyzed against 20 mM Tris-HCl (pH 8.0). Miniature MaSp1 proteins were released from the tags by proteolytic cleavage using a thrombin:fusion protein ratio of 1:1000 (w/w) at room temperature. The cleavage reaction was performed at a fusion protein concentration of 0.6−2 mg/mL in a tube that was gently wagged. Shorter fibers (1−10 cm) were made in 15 mL Falcon tubes (l = 116 mm, Ø = 15 mm) filled with 3 mL of protein solution. A longer glass

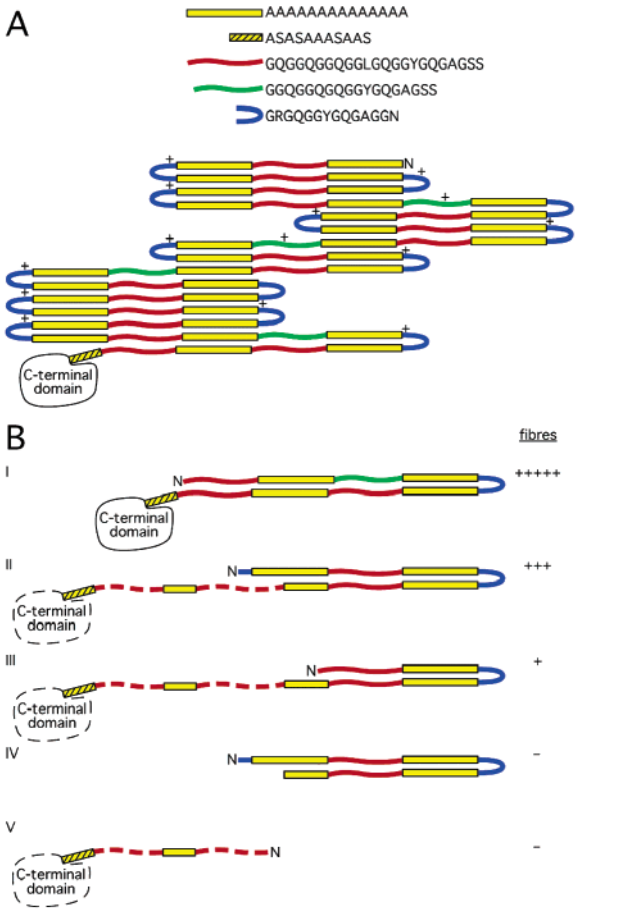

Figure 1. Composition of *E. australis* MaSp1 and of recombinant miniature MaSp1 constructs. (A) Consensus sequences of different segments and their hypothetical arrangement in the intact protein deduced from clone 2 are shown. Locations of positively charged residues are indicated. (B) Composition of recombinant constructs. Yellow boxes represent poly-Ala blocks. Red, green, and blue lines represent Gly-rich regions; see (A) for details. Construct I (MW 23.8 kDa) corresponds to the C-terminal part of *E. australis* MaSp1. Recombinant constructs II (MW 23.7 kDa) and III (MW 22.3 kDa) consist of repetitive segments from *Euprosthenops* MaSp1 (solid lines) joined to the non-repetitive C-terminal domain from *N. clavipes* (dotted lines). Recombinant construct IV (MW 10.1 kDa) consists only of an *Euprosthenops* repetitive segment, and construct V (MW 13.8 kDa) consists only of an *N. clavipes* non-repetitive C-terminal domain. The short poly-Ala blocks in constructs II−V contain 6 or 8 residues. Fiber formation ability for the different constructs is indicated (+++++, +++, +, and −). See text and Supporting Information, Figures 8 and 9, for details and exact amino acid sequences.

tube ($l = 1200$ mm, $Ø = 27$ mm) filled with 160 mL of protein solution was used for production of the longest fibers.

Samples from different stages during the process were analyzed by SDS-PAGE under both reducing and non-reducing conditions. Fiber pieces were vortexed with 3% SDS in formic acid and lyophilized before being dissolved in gel loading buffer.

Amino acid sequence analysis of the fibers was performed by 15 cycles of sequencer-assisted Edman degradation (Protein Analysis Centre, Karolinska Institute, Sweden).

Tensile Strength Measurements. The tensile properties of three fibers from construct I were characterized using a Zwick Roell Z2.5 material tester (Zwick, Ulm, Germany). All tests were performed in air at ambient conditions (20 °C and 52% relative humidity) using a loading speed of 10 mm/min. Fiber pieces were transferred directly from buffer, mounted, and subjected to two stretching−relaxation cycles. First, the fibers were elongated by pulling up to a force of 0.1 N. After relaxation, they were further drawn until a force of 0.25 N was applied. This treatment generated elongated homogeneous fibers with a diameter of approximately 80 μm as determined at five different points along each fiber by height measurements using a Mitutoyo IDC-112B instrument (Mitutoyo Corp., Tokyo, Japan) and as confirmed by scanning electron microscopy (SEM). The drawn fibers were cut into pieces, the ends of which were fixed between cardboard paper with glue (Loctite 420, Loctite, Göteborg, Sweden). Fiber samples were then fixed in the grips of the material tester, straightened, and stretched until they broke. Stress−strain curves were constructed using the initial cross-sectional area of the predrawn fiber, assuming a circular cross section.

Macroscopic Images. Fibers in aqueous solvent were placed in glass dishes and photographed using a Nikon D50 or a Ricoh Caplio G4 wide digital camera.

SEM. Fiber pieces from construct I, before and after stretch−relaxation cycles, were applied on SEM stubs and air-dried overnight. The samples were vacuum-coated with a 6 nm layer of gold and palladium. Specimens were observed and photographed with a LEO 1550 FEG microscope (Carl Zeiss, Oberkochen, Germany) using an acceleration voltage of 10 kV.

Circular Dichroism (CD) Spectroscopy. Fibers were washed in 20 mM phosphate buffer (pH 7) and suspended by vigorous vortexing in 2% SDS in the same buffer. CD spectra from 250 to 190 nm were recorded at 22 °C in a 0.1 cm path length quartz cuvette using a J-810 spectropolarimeter (Jasco, Tokyo, Japan). The scan speed was 50 nm/min, response time 2 s, acquisition interval 0.1 nm, and bandwidth 1 nm. The spectrum shown is an average of three consecutive scans.

Cell Experiments. Approximately 0.5 cm long pieces of fibers from construct I were adsorbed to the bottom of 6-well microtiter plates by letting them dry from a small volume of buffer. The fibers stayed attached to the surface when cell growth media was added. HEK 293 cells were then seeded and allowed to grow for a total of 6 days.

Results

Analysis of Structural Properties of *Euprosthenops australis* MaSp1 in Relation to Fiber Formation. Because of the attractive properties of *Euprosthenops* dragline silk, a cDNA library from *Euprosthenops australis* major ampullate glands was constructed. From this library, a 3.8-kb clone encoding a 1207 amino acid fragment of MaSp1, containing 68 alanine- and glycine-rich blocks and a C-terminal non-repetitive domain, was derived (see Figure 1A and Supporting Information, Figures 8 and 9, for sequences of repetitive and non-repetitive parts).

Spidroin polypeptides in solution have been reported to fold by formation of hairpin structures, which direct the antiparallel β-sheet structure of the mature fiber.[33] Therefore, patterns compatible with the formation of hairpin structures were searched for in the *E. australis* MaSp1 polypeptide. The Ala-rich segments are unlikely candidates for turn formation because they are predicted to form helical structures in solution and are believed to constitute the β-sheets in the fiber.[6,11] Three related but distinct types of Gly-rich segments can be identified in the *E. australis* MaSp1 polypeptide (Figure 1 and Supporting Information, Figure 8). The most common Gly-rich repeat contains 23−24 residues, while a less abundant variant contains 18 residues. Both of these Gly-rich segments generally lack charged residues. In contrast, the shortest Gly-rich segment (14 amino acid residues) contains a positively charged residue and has a unique GRGQG segment at the N-terminal end and a GN dipeptide segment at the C-terminal end.

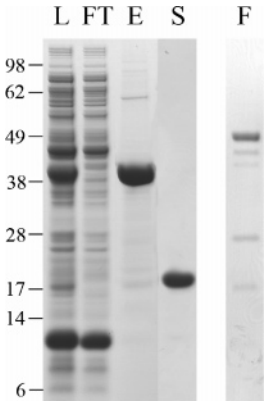

Figure 2. Purity of fusion protein and fiber protein composition. SDS-PAGE of whole cell lysates (lane L), flow-through from affinity column (lane FT), eluate from affinity column (lane E), soluble fraction after fiber formation is complete (lane S), and a fiber dissolved in formic acid (lane F). Migration of molecular size markers is indicated to the left.

Using a recently described algorithm for turn predictions,[31] the shortest Gly-rich segments show a likelihood for formation of type-II β-turns, while the two longer Gly-rich segments are predicted to form coil structures. The high content of GGX triplets in the longest Gly-rich segments suggests that they can form 3_1-helix structures, as described for GGX-rich segments of dragline silk from *N. edulis*.[34] The repetitive nature of the spidroin amino acid sequences implies an equally repetitive nature of the folding pattern. Taken together, these observations result in a hypothetical MaSp1 polypeptide arrangement shown in Figure 1A. Conformations, wherein alternative intramolecular interactions take place, are also possible. It is notable that in the model in Figure 1A the positively charged residues almost invariably are located in the proposed turn structures.

Macroscopic Fibers from Recombinant Miniature MaSp1 Proteins. From the pattern of the repetitive region of the *E. australis* MaSp1 protein, a sequence motif that consists of four poly-Ala/Gly-rich co-repeats, with a central turn, could be discerned (Figure 1, construct I). With the initial ambition to study structural properties, this motif followed by the non-repetitive C-terminal domain was expressed as a soluble thioredoxin/His-tag/S-tag fusion protein in *E. coli* and purified by immobilized metal ion affinity chromatography. This process yields about 40 mg/L culture of fusion protein with above 90% purity as judged by SDS-PAGE (Figure 2, lane E), which is stable for weeks without significant precipitation.

In contrast to the stable fusion protein, the miniature spidroin spontaneously polymerizes into macroscopic fibers after release from the fusion tag (Figure 3A). The fibers are formed at the air−liquid interface along the tube, starting at both ends and approaching the middle. Fiber formation could be observed by the naked eye within 10 min of incubation, and after 5 h no further visible fiber growth occurred. In this manner, fibers twice as long as the tube used, thus exceeding 1 m in length, can be

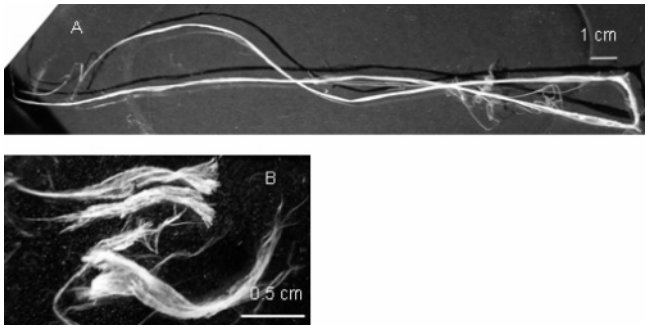

Figure 3. Macroscopic appearance of fibers. (A) Fibers formed from a miniature version of *E. australis* MaSp1 (construct I in Figure 1B). (B) Fibers formed from a hybrid miniature MaSp1, containing repetitive domains from *E. australis* and a non-repetitive domain from *N. clavipes* (construct II in Figure 1B).

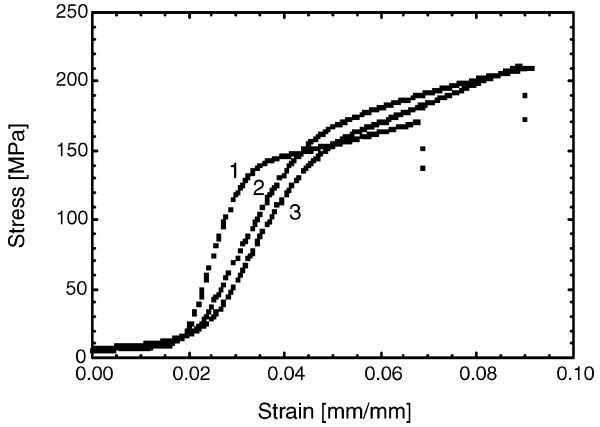

Figure 4. Tensile strength of double drawn fibers from construct I. The stress values are normalized to the initial cross-sectional area of the fiber. The strain corresponds to dL/L_0, where L_0 is the initial length of the fiber and dL is the change in fiber length. The stress−strain curves for three different samples, numbered 1−3, are shown.

produced. Fibers were easily detached from the tube and then washed with buffer and subjected to N-terminal amino acid sequence analysis, which showed only the sequence of the MaSp1 protein without the fusion tag. In line with this, SDS-PAGE analysis of a fiber dissolved in formic acid shows only monomeric and oligomeric forms of the recombinant MaSp1 (Figure 2, lane F). Moreover, only the fusion partner can be found in the supernatant after fiber formation (Figure 2, lane S), indicating that the miniature spidroin efficiently polymerizes into fibers.

These unexpected findings prompted further analysis of the structural requirements for fiber formation. The fiber-forming ability of different constructs, expressed and purified as for the initial miniature spidroin (construct I), is summarized in Figure 1B. Construct II contains three *Euprosthenops* MaSp1 poly-Ala/Gly-rich co-repeats, which are very similar to those in construct I linked to a non-repetitive C-terminal part of a *Nephila* MaSp1 (see Supporting Information, Figure 10). The shorter constructs, denoted III, IV, and V, are derived from construct II, as shown in Figure 1B. Construct II gave rise to fibers of about 2 cm in length (Figure 3B), whereas construct III formed just a few short (millimeter) fibers. Construct IV, which lacks the non-repetitive C-terminal domain, formed amorphous aggregates but no fibers. The non-repetitive C-terminal domain alone (construct V) remained soluble and did not form any fibers either. From these results, it can be concluded that minimal requirements for prominent fiber formation are four poly-Ala/Gly-rich co-repeats and a non-repetitive C-terminal domain. Such a miniature spidroin is estimated to be about 10% of the length of native MaSp1.

Characterization of Recombinant Spidroin Fibers. To generate a homogeneous silk thread suitable for tensile testing, the fibers were elongated using stretch−relaxation cycles. Mechanical properties of three fibers were then examined using tensile tests performed to yield stress−strain curves (Figure 4). The initial region of the curves should be interpreted with care, due to difficulties in mounting the fibers sufficiently straightened. The tensile strength of double drawn fibers of construct I measured approximately 0.2 GPa (171, 210, 212 MPa, respectively, for the three fibers in Figure 4). The elastic modulus was estimated to be approximately 7 GPa (9.1, 6.8, 6.1 GPa, respectively, for the three fibers). The average yielding stress was 150 MPa (139, 168, 151 MPa, respectively, for the three fibers).

The microscopic architecture of the fibers was analyzed via scanning electron microscopy (SEM) (Figure 5). The spontaneously formed fibers have a homogeneous flattened appearance and a width of up to several hundred micrometers, while the height measures some 10 μm (Figure 5A,B).

After the fibers had been subjected to stretch−relaxation cycles, they adopt a more compact shape with a substructure of tightly aligned fibrils (Figure 5C−F). The appearance of cut or fractured surfaces (Figure 5E,F) further attests to the compactness of the fiber.

Circular dichroism (CD) spectra of suspensions of construct I or II fibers displayed a single minimum at 220 nm and a maximum at 193 nm (Figure 6). These features indicate a substantial fraction of β-sheet structure. The red-shift of the minimum for the fiber spectrum as compared to that of a pure β-sheet (217 nm) and the rather low 193/220 ratio suggest that helical and turn structures may also be present. Preliminary X-ray diffraction studies of the fibers likewise indicate β-sheet structure (not shown). SEM, CD, and X-ray analysis of the spontaneously formed fibers described herein thus shows morphology and secondary structures similar to those of native or regenerated spider silk fibers.[35−38]

One common way of determining the biocompatibility of a novel material is by cohabitation with cells in tissue culture. Here, human embryonic kidney (HEK) 293 cells were found to survive and proliferate in the presence of recombinant silk fibers formed from construct I. The cells grew closely along the fiber edges and also under partly detached fibers (Figure 7). After 6 days, the fibers were carefully detached from the plastic surface, and it was evident that layers of cells were physically attached to the fibers.

Discussion

During the last 10 years, several attempts have been made to produce recombinant spidroins to generate artificial silk for biomedical and other purposes. Large-scale protein production is necessary to allow generation of man-made, high-performance silk fibers. The very long and repetitive nature of spidroin sequences, however, has complicated these efforts. High expression levels of recombinant dragline spidroins have been obtained; a synthetic gene-derived dragline spidroin was expressed in *Pichia pastoris* at levels up to 1 g/L.[24] However, only about 15% of the protein was found in the soluble fraction, and purity was an issue. Expression of MaSp analogues from *N. clavipes* in *E. coli* to form fibers has also been reported.[22,39,40] However, in these cases, solubility problems forced the protein

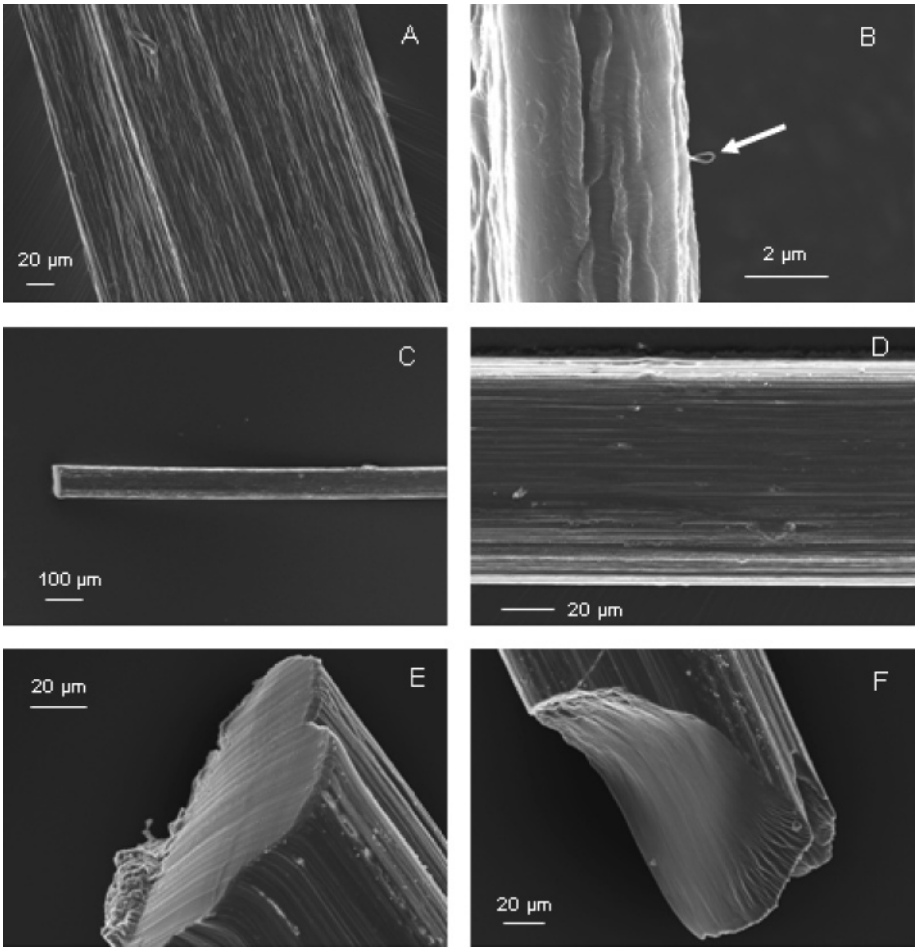

Figure 5. Scanning electron micrographs of recombinant fibers from construct I. (A,B) Spontaneously formed fibers. The close-up image (B) shows the fibrillar substructure. The small fibril that bulges out (arrow) has a width of about 300 nm. (C−F) Fibers after two stretching−relaxation cycles. (C) and (D) show the same fiber at different magnifications. (E) shows a cut fiber end, and (F) shows a point of breakage after tensile testing.

purification procedure to include the use of denaturing agents. An artificial spinning procedure, including a coagulation step, was introduced to obtain fibers from the redissolved and denatured proteins.[39,40] In a similar manner, another MaSp analogue has been expressed in mammalian cells and spun into fibers.[25] Also, in this case, protein purification was partly performed in the presence of urea because protein precipitation was significant, and artificial spinning including coagulation was used.

The data presented herein define a minimal *Euprosthenops* MaSp1 motif, consisting of four poly-Ala/Gly-rich blocks connected to a non-repetitive C-terminal domain, which is sufficient to form macroscopic silk-like fibers. By fusion of this motif to thioredoxin, expression of soluble protein in *E. coli* and high yield purification is obtained. This new approach allows production of a nondenatured protein and spontaneous fiber formation. After proteolytic removal of the fusion partner, generation of meter-long fibers is achieved within a few hours under physiological conditions. Fibers formed using this procedure resemble native spider silk regarding microscopic appearance and dominant secondary structure.

The fibers from our miniature spidroin are spontaneously formed but still as strong (∼0.2 GPa) as fibers that have been spun from redissolved spider silk material,[37] or from a recombinant MaSp2 analogue,[25] and, for example, tendons,[1] but they are weaker than artificially reeled dragline silk (∼0.8 GPa for *Araneus* and *Nephila* and ∼1.5 GPa for *Euprosthenops*[17]). The elastic modulus and yielding stress of the recombinant fibers, about 7 GPa and 150 MPa, respectively, are, however, comparable to those of native *Nephila* spider silk but lower than those of *Euprosthenops* dragline silk.[3,41] The lower strength of the self-assembled recombinant fibers as compared to native dragline silk is probably caused by several factors, such as the comparatively small size of the miniature spidroin, the absence of MaSp2 in the recombinant fiber, and the fact that a spinning procedure was not used. Modification of the procedure for fiber formation, for example by introduction of spinning, will likely affect the mechanical properties of the miniature spidroin fibers, thereby possibly allowing generation of a variety of fibers.

Native dragline silk that is dissolved in a strong chaotropic agent forms β-sheet structures and can be artificially spun into filaments after removal of the denaturing milieu.[37,38] Upon expression of a recombinant MaSp1-like protein in insect cells (i.e., under nondenaturing conditions), spontaneous formation of microscopic filaments within these cells has been reported.[28] It is here shown that nondenatured miniature spidroins can spontaneously form fibers in vitro. These observations indicate that the ability to assemble into fibers is determined by the spidroin amino acid sequence and conformation. However, the introduction of a spinning procedure can allow fiber formation also from denatured spidroins. The spinning procedure apparently influences the properties of the fiber as well.[3]

The data presented herein also show that only a small fraction of the spidroin sequence need to be present to dictate fiber formation. Moreover, a species hybrid containing a *Euprosthenops* repetitive domain and a *Nephila* non-repetitive C-

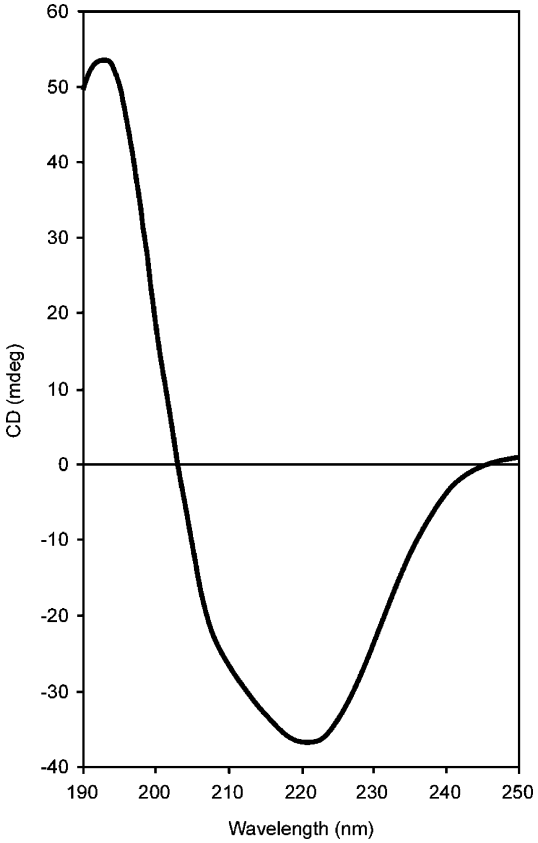

Figure 6. CD spectrum of fiber. Fibers from construct II suspended in 2% SDS in 20 mM phosphate buffer, pH 7. A similar spectrum was obtained from construct I fibers.

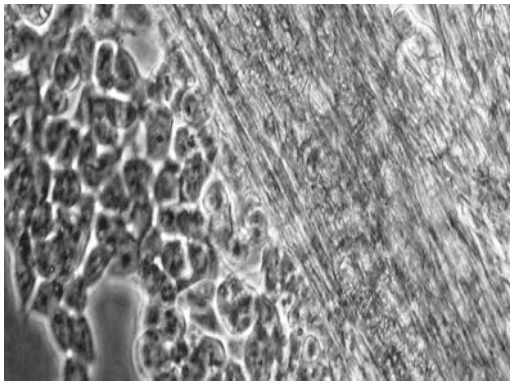

Figure 7. HEK 293 cells grown in the presence of recombinant fibers. The fiber covers the upper right-hand side of the figure. Cells are seen attached to the edge of the fiber, and also grow under the fiber.

terminal domain forms fibers as well, indicating that the fiber-forming potential of this motif is robust. The longest spontaneously formed fibers were derived from a motif containing four co-repeats followed by the non-repetitive C-terminal domain (construct I). Construct II with three such poly-Ala/Gly-rich repeats gave rise to significantly shorter fibers. The exact composition of the repeats, in particular the Gly-rich repeats, and the origin of the C-terminal domain are different in construct II as compared to those in construct I (Figure 1B). Exactly how the differences between constructs I and II influence the ability to form fibers remains to be determined. The full function of the C-terminal domain has not been established yet, although a potential role for increasing solubility and/or in the formation of the final structure of the silk fibers has been suggested.[12,13,25,42] The result presented herein shows that only constructs that contain both poly-Ala/Gly-rich regions and the C-terminal domain form fibers, supporting a crucial role for the C-terminal domain in the formation of silk fibers.

For biomedical applications, fibers also need to be biocompatible. A requirement for this to be possible is to ensure that no harmful substances are released from the final product. The recombinant fibers described herein support growth of HEK cells. Moreover, the cells are able to attach to the fiber, suggesting that it may function as a mediator of anchorage dependence. Large-scale production of recombinant miniature spidroins is currently attempted. Moreover, interactions with primary human cell cultures and in vivo biocompatibility of the fibers are under investigation.

In conclusion, we have identified a miniature spidroin motif that can be readily produced in bacteria and thereafter induced to spontaneously form meter-long fibers. For the first time, we show that neither a spinning procedure nor an in vivo milieu is needed for silk formation. The fibers are formed without the use of chaotropic agents, organic solvents, or change in pH throughout the process. Such fibers not only possess favorable mechanical properties but also allow cell growth, proliferation, and attachment. This strategy for spidroin production and fiber formation provides a novel alternative for the development of biomaterials.

Acknowledgment. S.G. and A.R. contributed equally to this work. We thank Simon McQueen-Mason, York University, for providing MaSp1 clones, Astri and John Leroy for help with collecting spiders, and Erika Storckenfeldt and Christine Ortlepp in the laboratory of Fritz Vollrath, Oxford University, for dissecting spider glands. We also thank Torbjörn Mathisen and Henrik Magnusson at RADI Medical Systems AB for help with mechanical testing, Björn Atthoff for scanning electron microscopy, and Louise Serpell for X-ray analysis. G.H. was funded by the Agricultural Functional Genomics program, Swedish University of Agricultural Sciences, Uppsala. This study was supported by a European Commission grant "Spiderman" contract no. G5RD-CT-2002-00738 and the Swedish Research Council. Sequence data have been submitted to the EMBL database under accession no. AJ973155.

Supporting Information Available. Molecular organization of the repetitive part of *Euprosthenops australis* MaSp1 clone 2 (Figure 8), amino acid sequences of expressed miniature MaSp1 proteins (Figure 9), and alignment of MaSp1 C-terminal domains from *Euprosthenops* sp., *Nephila clavipes* P19837, and *Euprosthenops australis* (Figure 10). This material is available free of charge via the Internet at http://pub.acs.org.

References and Notes

(1) Gosline, J. M.; Guerette, P. A.; Ortlepp, C. S.; Savage, K. N. *J. Exp. Biol.* **1999**, *202*, 3295−3303.
(2) Vollrath, F.; Barth, P.; Basedow, A.; Engstrom, W.; List, H. *In Vivo* **2002**, *16*, 229−234.
(3) Vollrath, F.; Knight, D. P. *Nature* **2001**, *410*, 541−548.
(4) Hinman, M. B.; Jones, J. A.; Lewis, R. V. *Trends Biotechnol.* **2000**, *18*, 374−379.
(5) Xu, M.; Lewis, R. V. *Proc. Natl. Acad. Sci. U.S.A.* **1990**, *87*, 7120−7124.
(6) Hinman, M. B.; Lewis, R. V. *J. Biol. Chem.* **1992**, *267*, 19320−19324.
(7) Mello, C. M.; Senecal, K.; Yeung, B.; Vouros, P.; Kaplan, D. In *Silk polymers. Materials science and biotechnology*; Kaplan, D., et al., Eds.; American Chemical Society: Washington, DC, 1994; pp 67−79.
(8) Jackson, C.; O'Brien, J. P. *Macromolecules* **1995**, *28*, 5975−5977.
(9) Sponner, A.; Schlott, B.; Vollrath, F.; Unger, E.; Grosse, F.; Weisshart, K. *Biochemistry* **2005**, *44*, 4727−4736.
(10) Sponner, A.; Unger, E.; Grosse, F.; Weisshart, K. *Nat. Mater.* **2005**, *4*, 772−775.

(11) Simmons, A. H.; Michal, C. A.; Jelinski, L. W. *Science* **1996**, *271*, 84−87.
(12) Sponner, A.; Unger, E.; Grosse, F.; Weisshart, K. *Biomacromolecules* **2004**, *5*, 840−845.
(13) Huemmerich, D.; Helsen, C. W.; Quedzuweit, S.; Oschmann, J.; Rudolph, R.; Scheibel, T. *Biochemistry* **2004**, *43*, 13604−13612.
(14) Challis, R. J.; Goodacre, S. L.; Hewitt, G. M. *Insect Mol. Biol.* **2006**, *15*, 45−56.
(15) Motriuk-Smith, D.; Smith, A.; Hayashi, C. Y.; Lewis, R. V. *Biomacromolecules* **2005**, *6*, 3152−3159.
(16) Rising, A.; Hjalm, G.; Engstrom, W.; Johansson, J. *Biomacromolecules* **2006**, *7*, 3120−3124.
(17) Madsen, B.; Shao, Z. Z.; Vollrath, F. *Int. J. Biol. Macromol.* **1999**, *24*, 301−306.
(18) Shao, Z.; Vollrath, F. *Polymer* **1999**, *40*, 1799−1806.
(19) Pouchkina-Stantcheva, N. N.; McQueen-Mason, S. J. *Comp. Biochem. Physiol., Part B: Biochem. Mol. Biol.* **2004**, *138*, 371−376.
(20) Prince, J. T.; McGrath, K. P.; DiGirolamo, C. M.; Kaplan, D. L. *Biochemistry* **1995**, *34*, 10879−10885.
(21) Lewis, R. V.; Hinman, M.; Kothakota, S.; Fournier, M. J. *Protein Expression Purif.* **1996**, *7*, 400−406.
(22) Fahnestock, S. R.; Irwin, S. L. *Appl. Microbiol. Biotechnol.* **1997**, *47*, 23−32.
(23) Arcidiacono, S.; Mello, C.; Kaplan, D.; Cheley, S.; Bayley, H. *Appl. Microbiol. Biotechnol.* **1998**, *49*, 31−38.
(24) Fahnestock, S. R.; Bedzyk, L. A. *Appl. Microbiol. Biotechnol.* **1997**, *47*, 33−39.
(25) Lazaris, A.; Arcidiacono, S.; Huang, Y.; Zhou, J. F.; Duguay, F.; Chretien, N.; Welsh, E. A.; Soares, J. W.; Karatzas, C. N. *Science* **2002**, *295*, 472−476.
(26) Scheller, J.; Guhrs, K. H.; Grosse, F.; Conrad, U. *Nat. Biotechnol.* **2001**, *19*, 573−577.
(27) Williams, D. *Med. Device Technol.* **2003**, *14*, 9−11.
(28) Huemmerich, D.; Scheibel, T.; Vollrath, F.; Cohen, S.; Gat, U.; Ittah, S. *Curr. Biol.* **2004**, *14*, 2070−2074.
(29) Wilson, D.; Valluzzi, R.; Kaplan, D. *Biophys. J.* **2000**, *78*, 2690−2701.
(30) LaVallie, E. R.; DiBlasio, E. A.; Kovacic, S.; Grant, K. L.; Schendel, P. F.; McCoy, J. M. *Biotechnology (N.Y.)* **1993**, *11*, 187−193.
(31) Fuchs, P. F.; Alix, A. J. *Proteins* **2005**, *59*, 828−839.
(32) Henke, W.; Herdel, K.; Jung, K.; Schnorr, D.; Loening, S. A. *Nucleic Acids Res.* **1997**, *25*, 3957−3958.
(33) Peng, X.; Shao, Z.; Chen, X.; Knight, D. P.; Wu, P.; Vollrath, F. *Biomacromolecules* **2005**, *6*, 302−308.
(34) van Beek, J. D.; Hess, S.; Vollrath, F.; Meier, B. H. *Proc. Natl. Acad. Sci. U.S.A.* **2002**, *99*, 10266−10271.
(35) Seidel, A.; Liivak, O.; Jelinski, L. W. *Macromolecules* **1998**, *31*, 6733−6736.
(36) Jelinski, L. W.; Blye, A.; Liivak, O.; Michal, C.; LaVerde, G.; Seidel, A.; Shah, N.; Yang, Z. *Int. J. Biol. Macromol.* **1999**, *24*, 197−201.
(37) Seidel, A.; Liivak, O.; Calve, S.; Adaska, J.; Ji, G.; Yang, Z.; Grubb, D.; Zax, D. B.; Jelinski, L. W. *Macromolecules* **2000**, *33*, 775−780.
(38) Shao, Z.; Vollrath, F.; Yang, Y.; Thogersen, H. C. *Macromolecules* **2003**, *36*, 1157−1161.
(39) OBrien, J. P.; Fahnestock, S. R.; Termonia, Y.; Gardner, K. H. *Adv. Mater.* **1998**, *10*, 1185−1195.
(40) Arcidiacono, S.; Mello, C. M.; Butler, M.; Welsh, E.; Soares, J. W.; Allen, A.; Ziegler, D.; Laue, T.; Chase, S. *Macromolecules* **2002**, *35*, 1262−1266.
(41) Vollrath, F.; Madsen, B.; Shao, Z. *Proc. Biol. Sci.* **2001**, *268*, 2339−2346.
(42) Ittah, S.; Cohen, S.; Garty, S.; Cohn, D.; Gat, U. *Biomacromolecules* **2006**, *7*, 1790−1795.

BM070049Y